Contribution from the Department of Chemistry,
The University of Houston—University Park, Houston, Texas 77004

Electroreduction of the Dioxygen Adduct of Rhodium Tetraphenylporphyrin: (TPP)Rh(O_2)

J. E. Anderson, C.-L. Yao, and K. M. Kadish*

Received December 28, 1985

The electroreduction of (TPP)Rh(O_2), where TPP is the dianion of tetraphenylporphyrin, was studied in benzonitrile, tetrahydrofuran, and methylene chloride by cyclic voltammetry, spectroelectrochemistry, and ESR spectroscopy. Two reductions were observed. The first reduction was irreversible in that the electron transfer was followed by a chemical reaction. The product of this chemical reaction depended upon the solvent. In benzonitrile and THF, the one-electron reduction of (TPP)Rh(O_2) resulted in the formation of a Rh(II) dimer. In CH_2Cl_2, a rhodium–carbon σ-bonded species was formed. Triphenylphosphine was added to solutions of (TPP)Rh(O_2), and the ligand addition reaction was followed by both cyclic voltammetric and spectrophotometric techniques. An overall two-step substitution reaction occurred, and stability constants of log K_1 = 5.52 and log K_2 = 2.04 were obtained in CH_2Cl_2 for the successive addition of two triphenylphosphine molecules to the rhodium porphyrin unit to form (TPP)Rh(O_2)[$P(Ph)_3$] and (TPP)Rh[$P(Ph)_3]_2^+$. Smaller values for the formation constants were observed in THF and benzonitrile, and in this latter solvent, only the first ligand addition reaction was observed.

Introduction

Dioxygen adducts of rhodium octaethylporphyrin and tetraphenylporphyrin complexes have been reported in the literature.[1-3] These five-coordinate species are represented as (P)Rh(O_2) where P is the dianion of octaethylporphyrin (OEP) or tetraphenylporphyrin (TPP). These compounds have a 17-electron metal center and hence are paramagnetic. An ionic model has been assigned for the Rh–O bond in these species on the basis of ESR experiments.[3] Thus, the compound is described as an Rh^{III}–O_2^- species.

While the reaction chemistry of different types of rhodium macrocycles has been examined in general,[4-10] few studies have been performed on the rhodium porphyrins containing bound oxygen. Some alkylphosphine and alkyl phosphite donor complexes of (P)Rh(O_2) have been synthesized, but no electrochemistry for these types of complexes has ever been reported. Thus, one purpose of this paper is to present such data.

Two papers have recently appeared on the electroreduction of the rhodium porphyrin system.[11,12] The one-electron reduction of Rh(III) porphyrin species results in the formation of a reactive monomeric Rh(II) species that can dimerize[11] or, in some cases, react to form a rhodium–carbon bond.[13] However, the axial ligands in the rhodium porphyrin system have a dramatic impact on the electrochemical behavior. We wish to report the electroreduction of (TPP)Rh(O_2) and show that the reduction of the dioxygen complex is very similar to that of (TPP)Rh[$NH(CH_3)_2]_2^+Cl^-$ and (TPP)Rh[$NH(CH_3)_2$]Cl. Spectrophotometric titrations of (TPP)Rh(O_2) with triphenylphosphine were also performed and show that a two-step substitution reaction occurs with the eventual formation of (TPP)Rh[$P(Ph)_3]_2^+$ in the second step. Equilibrium constants were spectrophotometrically determined for the ligand substitution reactions. The titration of (TPP)Rh(O_2) with triphenylphosphine was also followed by cyclic voltammetry, and the two different triphenylphosphine adducts were examined by ESR spectroscopy. Finally, the electrochemistry of the rhodium porphyrin system as a function of axial ligand is discussed.

Experimental Section

Instrumentation and Methods. All electrochemical measurements, with the exception of the spectroelectrochemical experiments, were performed with Schlenk methodologies. Solutions that had been bulk-electrolyzed for ESR measurements were transferred under an inert atmosphere to ESR cells, adapted for Schlenk use, and then frozen with liquid nitrogen. Spectroelectrochemical measurements were performed with an electrochemical cell whose cell construction is reported in the literature.[14]

Spectrophotometric titrations were used to determine formation constants for the bonding of triphenylphosphine to (TPP)Rh(O_2). Stock solutions of the metalloporphyrin and ligand were prepared using typical metalloporphyrin concentrations of 10^{-5} M. Each spectrum was measured 2 min after addition of triphenylphosphine and monitored until no further changes were observed. This was to ensure equilibrium. Evaluation of the spectrophotometric data was performed by the Benesi–Hildebrandt method (B–H method),[15,16] and the final formation constants were calculated by a linear-least-squares program.

Cyclic voltammetric measurements were obtained at a Pt electrode disk with an EG&G Princeton Applied Research Model 174A/175 polarographic analyzer/potentiostat coupled with an EG&G Model 9002A X-Y recorder. Potentials were all measured relative to a saturated calomel electrode (SCE). This electrode was separated from the bulk of the solution by a fritted-glass-disk junction. Bulk controlled-potential coulometry was performed on an EG&G Princeton Applied Research Model 174 potentiostat and Model 179 coulometer system that was coupled with a Princeton Applied Research Model RE-0074 time base X-Y recorder. Thin-layer spectroelectrochemical measurements were made with an IBM 225/2A voltammetric analyzer that was coupled with a Tracor Northern 1710 spectrometer/multichannel analyzer. IR spectra were measured on a Perkin-Elmer 1330 infrared spectrophotometer using CsI cells. UV–visible spectra were recorded on an IBM Model 9430 UV–visible spectrophotometer. An IBM Model ED-100 electron spin resonance system was used to record ESR spectra.

Materials. All solvents used for electrochemistry and ligand addition were purified immediately before use. HPLC grade dichloromethane (CH_2Cl_2) was distilled from P_2O_5. Reagent grade benzonitrile (PhCN) was vacuum-distilled over P_2O_5. Spectroscopic grade tetrahydrofuran (THF) was distilled from P_2O_5 followed by distillation from sodium. Tetra-*n*-butylammonium perchlorate (TBAP) was purchased from Eastman Kodak Co., twice recrystallized from ethyl alcohol, and stored in a vacuum oven at 40 °C. Unless otherwise noted, 0.2 M TBAP was used for bulk solution electrolysis and spectroelectrochemical measure-

(1) James, B. R.; Stynes, D. V. *J. Am. Chem. Soc.* **1972**, *94*, 6225.
(2) Wayland, B.; Newman, A. *J. Am. Chem. Soc.* **1979**, *101*, 6472.
(3) Wayland, B.; Newman, A. *Inorg. Chem.* **1981**, *20*, 3093.
(4) Collman, J. P.; Brauman, J. I.; Madonik, A. M. *Organometallics* **1986**, *5*, 215.
(5) Collman, J. P.; Brauman, J. I.; Madonik, A. M. *Organometallics* **1986**, *5*, 310.
(6) Setsune, J. J.; Yoshida, Z.-I.; Ogoshi, H. *J. Chem. Soc., Perkin Trans. 1* **1982**, 983.
(7) Aoyama, Y.; Yoshida, T.; Sakuri, K.-I.; Ogoshi, H. *J. Chem. Soc., Chem. Commun.* **1983**, 478.
(8) Aoyama, Y.; Yoshida, T.; Sakurai, K.; Ogoshi, H. *Organometallics* **1986**, *5*, 168.
(9) Del Rossi, K. J.; Wayland, B. B. *J. Am. Chem. Soc.* **1985**, *107*, 7941.
(10) Van Voorhees, S. L.; Wayland, B. B. *Organometallics* **1985**, *4*, 1887.
(11) Kadish, K. M.; Yao, C.-L.; Anderson, J. E.; Cocolios, P. *Inorg. Chem.* **1985**, *24*, 4515.
(12) Kadish, K. M.; Anderson, J. E.; Yao, C.-L.; Guilard, R. *Inorg. Chem.* **1986**, *25*, 1277.
(13) Anderson, J. E.; Yao, C.-L.; Kadish, K. M. *Inorg. Chem.* **1986**, *25*, 718.
(14) Lin, X.-Q.; Kadish, K. M. *Anal. Chem.* **1985**, *57*, 1498.
(15) Benesi, H. A.; Hildebrand, J. H. *J. Am. Chem. Soc.* **1949**, *71*, 2703.
(16) Rose, N. J.; Drago, R. S. *J. Am. Chem. Soc.* **1959**, *81*, 6138.

0020-1669/86/1325-3224$01.50/0

Table I. Half-Wave and Peak Potentials (V vs. SCE) and UV–Visible Spectra of Various (TPP)Rh$(L)_2^+$ and (TPP)Rh$(O)_2$L Complexes

compd	solvent	E_p[a]	$E_{1/2}$	λ_{max}, nm ($\epsilon \times 10^{-3}$)		
(TPP)Rh(O_2)	CH_2Cl_2	−1.14	−1.40	418 (188)	534 (18.1)	574 (3.2)
	THF	−1.12	−1.84	418 (230)	531 (20.6)	565 (4.8)
	PhCN	−1.14	−1.93	428 (221)	538 (19.8)	573 (4.6)
(TPP)Rh(O_2)[$P(Ph)_3$][b]	CH_2Cl_2	−0.88	−1.50	437 (191)	546 (13.9)	582 (7.2)
	THF	−0.74		435 (203)	546 (13.9)	584 (8.0)
	PhCN	−0.84		438 (149)	556 (11.2)	597 (10.6)
(TPP)Rh[$P(Ph)_3$]$_2^+$[c]	CH_2Cl_2	−0.98	−1.54	444 (177)	553 (10.7)	595 (9.3)
	THF			445 (160)	554 (9.6)	596 (8.0)
(TPP)Rh[$NH(CH_3)_2$]$_2^+Cl^-$	CH_2Cl_2[d]	−1.07	−1.50	418 (322)	528 (30.1)	561 (6.5)
	THF[e]	−0.96	−1.83	419 (281)	529 (21.6)	562 (4.9)
	PhCN[e]	−1.06	−1.95	421 (272)	530 (25.0)	564 (5.8)

[a] Peak potential at a scan rate of 0.1 V/s. [b] Mole ratios of $P(Ph)_3$ to (TPP)Rh(O_2) of 40:1 in CH_2Cl, 40:1 in THF, and 80:1 in PhCN. [c] Mole ratios of $P(Ph)_3$ to (TPP)Rh(O_2) of 580:1 for electrochemical measurements and 10000:1 (~0.1 M $P(Ph)_3$) for spectroscopic measurements. [d] Reference 13. [e] Reference 11.

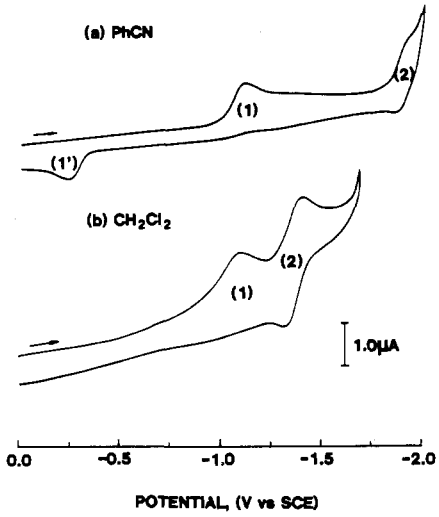

Figure 1. Cyclic voltammogram of (a) 7.4×10^{-4} M (TPP)Rh(O_2) in PhCN and (b) 8.4×10^{-4} M (TPP)Rh(O_2) in CH_2Cl_2 (0.1 M TBAP; scan rate 0.1 V/s).

ments while 0.1 M TBAP was used as supporting electrolyte for cyclic voltammetric measurements.

(TPP)Rh(O_2) was synthesized by the method of James[1] and was identified by UV–visible, IR, and ESR spectroscopy. The UV–visible spectra are reported in Table I as a function of solvent. The ESR spectrum was the same as that reported by both James[1] and Wayland.[2,3] The compound has g values (±0.002) of 2.082, 2.023, and 1.993 in PhCN and 2.087, 2.026, and 1.991 in frozen CH_2Cl_2 solutions.

Results and Discussion

Reduction of (TPP)Rh(O_2) in Benzonitrile and THF. A cyclic voltammogram of (TPP)Rh(O_2) in benzonitrile is shown in Figure 1a, and the potentials for the reductions are reported in Table I. Two reductions are observed in the potential range of PhCN. The first reduction (peak 1, Figure 1a) is not reversible, and at a scan rate of 0.1 V/s, $E_p = -1.14$ V in benzonitrile. As seen in Figure 1, the first reduction is not directly coupled to a reverse reoxidation peak. However, the shape and height of the first reduction peak are indicative of a diffusion-controlled one-electron transfer. The peak shape is given by $|E_p - E_{p/2}| = 60 \pm 10$ mV, and $i_p/v^{1/2}$ is constant. In addition, current integration gives a value of 1.0 ± 0.1 for the number of electrons transferred in the reduction. These data are consistent with an initial diffusion-controlled one-electron-reduction process that is followed by a rapid chemical reaction.

An oxidation peak occurs at $E_p = -0.24$ V in PhCN (Figure 1a, peak 1′) when the initial negative scan is reversed at potentials more negative than −1.20 V. A similar reoxidation peak occurs at −0.22 V in THF. This oxidation is not observed in CH_2Cl_2 (Figure 1b), nor is it observed in PhCN or THF if the scan is reversed before the first reduction peak. This clearly indicates that peak 1′ is due to one or more products formed from the first reduction. This same behavior was observed for (TPP)Rh[$NH(CH_3)_2$]$_2^+Cl^-$ and (TPP)Rh[$NH(CH_3)_2$]Cl in PhCN.[11] In fact, the potentials for peak 1′ are identical for all three compounds in PhCN, thus suggesting the same product is formed after the first reduction.

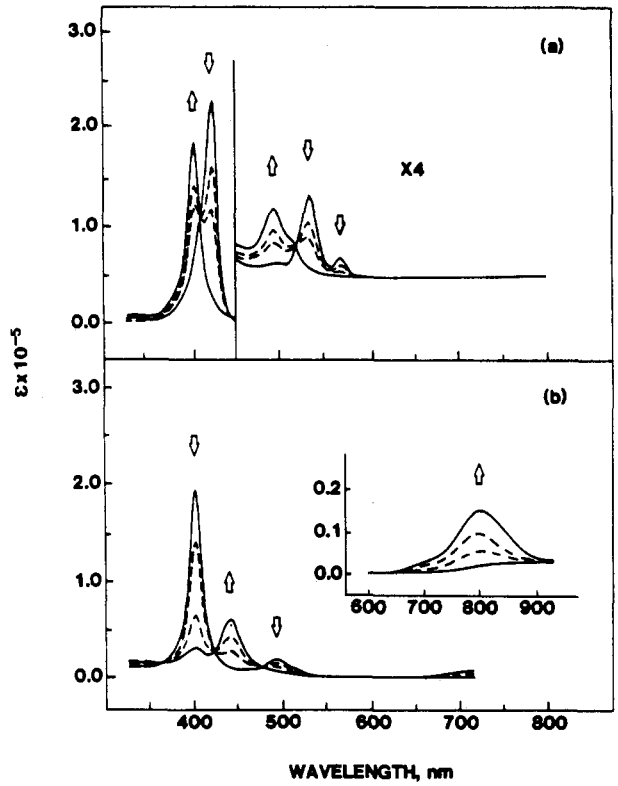

Figure 2. Electronic absorption spectra of (a) neutral and singly reduced (TPP)Rh(O_2) and (b) singly reduced and doubly reduced (TPP)Rh(O_2) in PhCN (0.2 M TBAP).

The electronic absorption spectrum of (TPP)Rh(O_2) is characterized by bands at 428, 538, and 573 nm in PhCN (see Table I). The Soret band of the compound shows a strong spectral dependence upon the solvent system. For instance, in THF and CH_2Cl_2 the Soret band is located at 418 nm. This suggests a solvent interaction of PhCN with the metal center and the probable formation of (TPP)Rh(O_2)(S) where S = PhCN. A solvent effect on spectra is not observed for (TPP)Rh[$NH(CH_3)_2$]$_2^+Cl^-$ and (TPP)Rh[$NH(CH_3)_2$]Cl (see Table I), which are already hexacoordinated.

The electronic absorption spectrum of (TPP)Rh(O_2) was monitored during controlled-potential reduction at −1.30 V, and the observed spectral changes are shown in Figure 2a for this reduction in PhCN. After the addition of one electron to (TPP)Rh$(O)_2$, the Soret band moves from 428 to 406 nm, and the bands at 538 and 573 nm disappear. At the same time there is a new band at 496 nm. Isosbestic points are observed at 413, 452, and 522 nm. A similar spectrum is observed after the first re-

Table II. UV–Visible Spectra of Reduced (TPP)Rh(O_2) in Various Solvents

solvent	electrode reacn	λ_{max}, nm ($\epsilon \times 10^{-3}$)		
PhCN	none	428 (221)	538 (19.8)	573 (4.6)
	1st redn[a]	406 (179)	496 (17.0)	
	2nd redn[b]	446 (57.1)	800 (14.8)	
THF	none	418 (230)	531 (20.6)	565 (4.8)
	1st redn[a]	404 (209)	496 (15.0)	
	2nd redn[b]	444 (63.1)	785 (6.0)	
CH_2Cl_2	none	418 (188)	534 (18.1)	574 (3.2)
	1st redn	414 (186.0)	523 (19.8)	598 (1.7)
	2nd redn	400 (79.1)	600 (8.5)	

[a] Reduction product formulated as $[(TPP)Rh]_2$. See ref 11. [b] Reduction product formulated as $[(TPP)Rh]_2^{2-}$. See ref 11.

duction of (TPP)Rh(O_2) in THF (see Table II). This spectrum is identical with the absorption spectrum of reduced (TPP)Rh-$[NH(CH_3)_2]_2^+Cl^-$ and (TPP)Rh$[NH(CH_3)_2]$Cl and thus suggests a similar product. The first reduction product of (TPP)Rh(O_2) is ESR silent, which is also observed for singly reduced (TPP)-Rh$[NH(CH_3)_2]_2^+Cl^-$ and (TPP)Rh$[NH(CH_3)_2]$Cl.

The first reduction of (TPP)Rh$[NH(CH_3)_2]_2^+Cl^-$ and (TP-P)Rh$[NH(CH_3)_2]$Cl is metal-centered and is followed by a fast chemical reaction. In benzonitrile, THF, and pyridine, the product of this reaction is $[(TPP)Rh]_2$.[11] Clearly, $[(TPP)Rh]_2$ is also formed following the one-electron reduction of (TPP)Rh(O_2) in benzonitrile and THF (see spectral data in Table II). Dimerization of (TPP)Rh is coupled with the loss of O_2^- so that the overall electrode reaction for peak 1 can be represented by eq 1.

$$(TPP)Rh(O_2) + e^- \rightarrow {}^1/_2[(TPP)Rh]_2 + O_2^- \qquad (1)$$

The second reduction of (TPP)Rh(O_2) occurs at −1.93 V in benzonitrile (peak 2, Figure 1a) and at −1.84 V in THF. This reduction involves a two-electron transfer to $[(TPP)Rh]_2$ as evidenced by the peak separation $|E_{pa} - E_{pc}| = 30 \pm 10$ mV. Upon reduction of $[(TPP)Rh]_2$, the Soret band at 406 nm drops in intensity and new bands appear at 446 and 800 nm (PhCN) or 444 and 785 nm (THF). These changes are shown in Figure 2b for electroreduction in PhCN, and the spectral changes are indicative of reduction at the porphyrin π-ring system. As expected, no ESR spectrum was observed for this two-electron-reduction product.

Similar room-temperature electrochemical behavior was observed for the reduction of (TPP)Rh(O_2) and (TPP)Rh$[NH(CH_3)_2]_2^+Cl^-$ in PhCN and THF (see Table I). However, there are some differences at low temperature. The reduction of (TPP)Rh$[NH(CH_3)_2]_2^+Cl^-$ is reversible in THF at −78 °C,[11] but cyclic voltammograms of (TPP)Rh(O_2) in THF at −78 °C do not give rise to a reversibility of the first reduction wave. Apparently, the reaction following reduction of the Rh center rapidly occurs, leaving the Rh(II) monomer, which can then dimerize as shown in reaction 1.

Reduction of (TPP)Rh(O_2) in Methylene Chloride. The chemistry of reduced (TPP)Rh(O_2) is different in methylene chloride. This is shown in Figure 1b. The first reduction is characterized by a broad, irreversible reduction wave at $E_p = -1.14$ V, and a new reversible wave is found at $E_{1/2} = -1.40$ V. The second wave is due to reduction of the chemical reaction product that is formed following the initial one-electron addition. The electrochemical properties of this reaction product are completely different from those of $[(TPP)Rh]_2$. The potential of $E_{1/2} = -1.40$ V is indicative of a Rh–carbon bonded species,[17] but the new species formed is not (TPP)Rh(CH_2Cl), which is formed when (TPP)Rh$[NH(CH_3)_2]_2^+Cl^-$ is reduced in CH_2Cl_2.[13] (TPP)Rh-(CH_2Cl) is reduced at −1.50 V. The UV–visible spectrum of the new species is also different from that of (TPP)Rh(CH_2Cl). The compound formed has absorption bands at 414, 523, and 598 nm (see Figure 3 and Table II) while (TPP)Rh(CH_2Cl) is characterized by bands at 422, 535, and 566 nm.

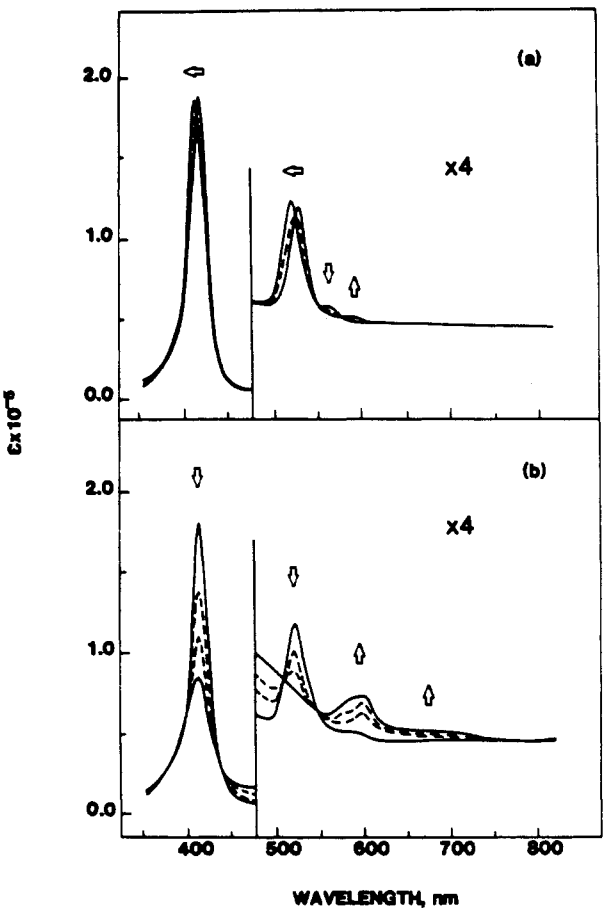

Figure 3. Electronic absorption spectra of (a) neutral and singly reduced (TPP)Rh(O_2) and (b) singly reduced and doubly reduced (TPP)Rh(O_2) in CH_2Cl_2 (0.2 M TBAP).

No ESR spectrum is obtained following bulk electrolysis of (TPP)Rh(O_2) at −1.30 V in CH_2Cl_2, but a strong free-radical signal is obtained following reduction at −1.60 V. This signal is characterized by a g value of 2.00 with a width of 32 G. The free-radical nature of the ESR signal indicates that reduction occurs at the porphyrin π-ring system, and this agrees with the UV–visible spectra (Figure 3b). During reduction the Soret band at 414 nm decreases in intensity and shifts to 400 nm while the bands at 523 and 598 nm also decrease in intensity. A new band is observed at 600 nm and is indicative of reduction at the porphyrin ring system. These spectral changes are summarized in Table II.

The product formed from the chemical reaction involving singly reduced (TPP)Rh(O_2) in CH_2Cl_2 has not been completely identified. The major difference between the final products of reduced (TPP)Rh$[NH(CH_3)_2]_2^+Cl^-$ and reduced (TPP)Rh(O_2) in methylene chloride appears to be a loss of reactive O_2^- in the latter case. Superoxide is known to react with methylene chloride[18] with the eventual formation of Cl^- and either $CH_2O_2^-$ or CH_2O. Therefore, it may be that one of these species is bonded to the product. However, characterization of the isolated compound after bulk electrolysis is inconclusive at this point.

Bonding of (TPP)Rh(O_2) by Triphenylphosphine. (TPP)Rh(O_2) will react in the presence of strong complexing ligands, resulting

(17) All (P)Rh(R) complexes investigated to date can be reversibly reduced by one electron in CH_2Cl_2. For example, this reaction occurs at −1.41 V for (TPP)Rh($COCH_3$) in CH_2Cl_2 (0.1 M TBAP) while (TPP)Rh-(CH_3) and (TPP)Rh(CH_2Cl) are reduced in this solvent (0.1 M TBAP) at −1.44 and −1.50 V, respectively.

(18) Sawyer, D. T.; Nanni, E. J.; Roberts, J. L. In *Electrochemical and Spectroelectrochemical Studies of Biological Redox Components*; Kadish, K. M., Ed.; American Chemical Society: Washington, DC, 1982.

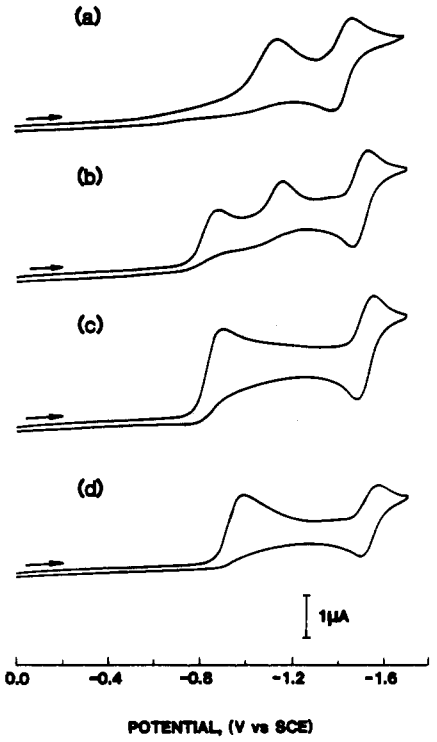

Figure 4. Cyclic voltammograms of 1.0×10^{-3} M (TPP)Rh(O_2) in CH_2Cl_2 (0.1 M TBAP) containing various concentrations of $P(Ph)_3$: (a) 0 equiv of $P(Ph)_3$; (b) 2 equiv of $P(Ph)_3$; (c) 40 equiv of $P(Ph)_3$; (d) 580 equiv of $P(Ph)_3$.

in the formation of (TPP)Rh$(L)_2^+$, where L is a neutral ligand. This is demonstrated by a titration of (TPP)Rh(O_2) with triphenylphosphine that was carried out in PhCN, THF, and CH_2Cl_2 and monitored by both cyclic voltammetry and UV–visible spectroscopy.

Figure 4 demonstrates the changes that occur in the cyclic voltammograms of (TPP)Rh(O_2) in CH_2Cl_2 upon the addition of triphenylphosphine. In the absence of triphenylphosphine, the cyclic voltammogram is characterized by an irreversible wave at $E_p = -1.14$ V and a reversible wave at $E_{1/2} = -1.40$ V (Figure 4a). Upon the addition of 2 equiv of triphenylphosphine, a new reduction wave is observed at $E_p = -0.88$ V. This is shown in Figure 4b. The current for this reduction increases as the concentration of triphenylphosphine is increased, and there is a simultaneous decrease in current of the peak at $E_p = -1.14$ V. This indicates the formation of a new species, assigned as (TPP)Rh(O_2)[$P(Ph)_3$]. At the same time, the second reduction has shifted from $E_{1/2} = -1.40$ V to $E_{1/2} = -1.52$ V, indicating complexation of the reduced product.

The shift to an easier first reduction of the rhodium complex reflects the bonding of the π-acid triphenylphosphine ligand and suggests either a stabilization of the initial Rh(II) reduction product or an increase in the rate of the chemical reaction following electron transfer. However, there is also a change in coordination geometry upon complexation with PPh_3, and this will effect the energy levels of the metal d orbitals. Since electron addition is to a molecular orbital consisting primarily of metal and axial ligand character, this geometrical change may also influence the observed reduction potential. The original first reduction wave at $E_p = -1.14$ V does not totally disappear until there is about a 20:1 molar ratio of triphenylphosphine to (TPP)Rh(O_2) in solution. This is demonstrated in Figure 4c, where the molar ratio is 40:1. Upon larger molar ratios, the wave at $E_p = -0.88$ V shifts to more negative potentials as shown in Figure 4d, where the mole ratio of triphenylphosphine to porphyrin is about 580:1. This shift toward negative values is due to replacement of O_2^- by triphenylphosphine, but the actual electrochemical mechanism is complicated by the fact that the peak potentials depend upon both ligation and the rates of any coupled chemical reactions.[19] Unfortunately, the solubility of triphenylphosphine in CH_2Cl_2 is close to 0.5 M at room temperature, and thus it was not possible to monitor additional shifts of E_p with further increases in the complexing ligand concentration.

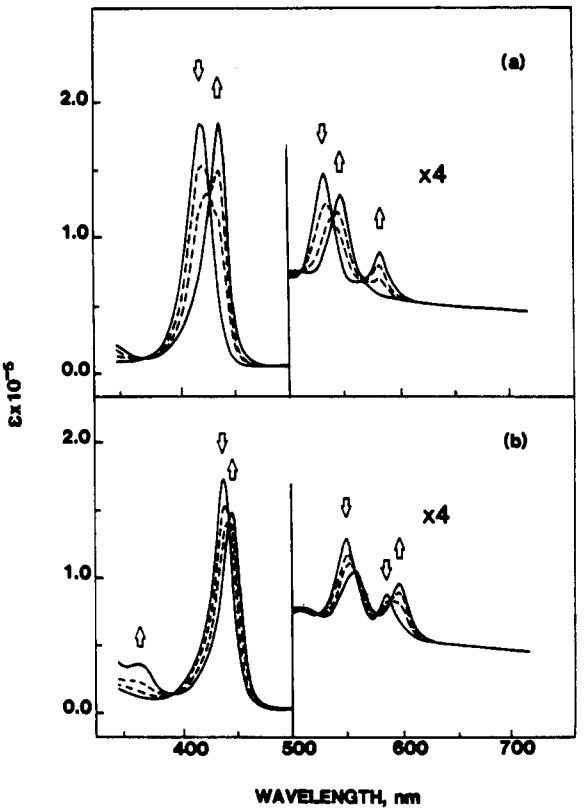

Figure 5. (a) Electronic absorption spectra of (TPP)Rh(O_2) in CH_2Cl_2 during the titration with $P(Ph)_3$ in CH_2Cl_2 (0.1 M TBAP). (b) Electronic absorption spectra of (TPP)Rh(O_2)[$P(Ph)_3$] in CH_2Cl_2 during the titration with $P(Ph)_3$ in CH_2Cl_2 (0.1 M TBAP).

Spectrophotometric monitoring of the titration confirms the formation of (TPP)Rh(O_2)[$P(Ph)_3$] and (TPP)Rh[$P(Ph)_3]_2^+$ in CH_2Cl_2. The formation of two different rhodium triphenylphosphine adducts is given by eq 2 and 3, where L = $P(Ph)_3$. Both of these reactions can be monitored by UV–visible spectroscopy in CH_2Cl_2 due primarily to the fact that solutions of (TPP)Rh(O_2) are much more dilute for UV–visible measurements ($\sim 10^{-5}$ M) than for cyclic voltammetric experiments ($\sim 10^{-3}$ M).

$$\text{(TPP)Rh}(O_2) + L \rightleftarrows \text{(TPP)Rh}(O_2)L \qquad (2)$$

$$\text{(TPP)Rh}(O_2)L + L \rightleftarrows \text{(TPP)Rh}(L)_2^+ + O_2^- \qquad (3)$$

Reaction 2 is complete after about 15 equiv of triphenylphosphine have been added to solutions of (TPP)Rh(O_2) in CH_2Cl_2. Reaction 3 is observed upon addition of more than 500 equiv of triphenylphosphine to this solution. A direct observation of O_2^- was not made in this reaction. The proposed replacement of O_2^- by triphenylphosphine is based on the fact that the addition of two triphenylphosphine ligands to (TPP)Rh(O_2) was demonstrated by both cyclic voltammetry and UV–visible spectroscopy. The triphenylphosphine monoadduct is characterized by bands at 437, 546, and 582 nm (see Table I), and the changes in the UV–visible spectrum of (TPP)Rh(O_2) during the titration are shown in Figure 5a. Three distinct isosbestic points are present at 370, 428, and 540 nm, thus indicating the formation of only one new species during the first part of the titration. Analyses of the spectral changes were carried out as a function of ligand concentration and led to a plot of the type shown in Figure 6a, from which a value of log $K_1 = 5.52$ is obtained in CH_2Cl_2.

(19) Values of E_p will shift in a positive direction as the rate constant for the following chemical reaction is increased. The exact magnitude of the shift will depend upon the order of the reaction, the magnitude of the rate constant, and for the reversible reactions, upon the equilibrium constant for the following chemical reaction.[20]

(20) Nicholson, R. S.; Shain, I. *Anal. Chem.* **1966**, *36*, 704.

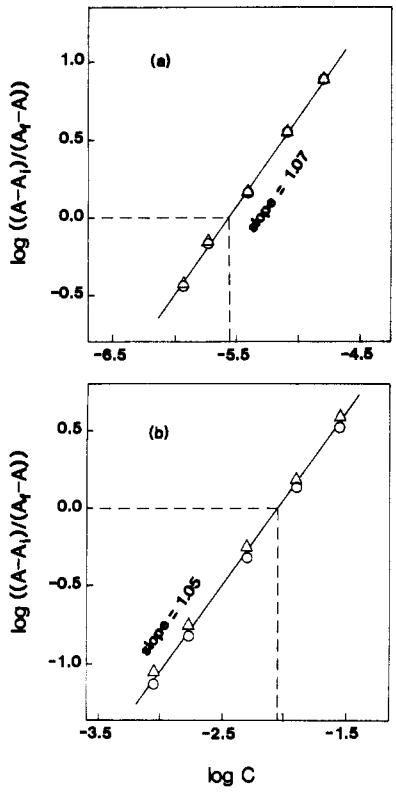

Figure 6. (a) Analysis of spectral data for the titration of $(TPP)Rh(O_2)$ with $P(Ph)_3$ in CH_2Cl_2. Wavelengths analyzed: 418 nm (○); 534 nm (△). (b) Analysis of spectral data for the titration of $(TPP)Rh(O_2)[P(Ph)_3]$ with $P(Rh)_3$ in CH_2Cl_2. Wavelengths analyzed: 437 nm (○), 546 nm (△).

Similar types of spectral changes were observed in THF and PhCN but only at larger ligand concentrations.

The first triphenylphosphine complex formed (reaction 2) has an ESR signal similar to that of $(TPP)Rh(O_2)$, but doublets are observed for the lines corresponding to g_2 and g_3. This same effect was observed upon the addition of tributyl phosphite to $(OEP)Rh(O_2)$ and triethyl phosphite to $(TPP)Rh(O_2)$.[3] The compounds formed in these reactions were shown to be $(OEP)Rh(O_2)[P(OBu)_3]$ and $(TPP)Rh(O_2)[P(OEt)_3]$. The splitting in the ESR spectra for these complexes was assigned as due to the ^{31}P nucleus. Values of A close to 21 G were reported for the $(OEP)Rh(O_2)[P(OBu)_3]$ complex while values of A close to 35 G were reported for the $(TPP)Rh(O_2)[P(OEt)_3]$ complex. In the case of the latter complex, the g_1 signal showed no hyperfine splitting.[3] In the present study, the ESR-active compound is assigned as $(TPP)Rh(O_2)[P(Ph)_3]$. The ESR spectrum is characterized in CH_2Cl_2 by absorbances at $g_1 = 2.084$ with $A(^{31}P) \sim 0$, $g_2 = 2.017$ with $A(^{31}P) = 3.31 \times 10^{-3}$ cm^{-1} (35.4 G), and $g_3 = 2.001$ with $A(^{31}P) = 3.28 \times 10^{-3}$ cm^{-1} (35.1 G). Similar ESR spectra were obtained for the triphenylphosphine monoadduct in THF and in PhCN.

Changes in the UV–visible spectrum upon formation of $(TPP)Rh[P(Ph)_3]_2^+$ from $(TPP)Rh(O_2)[P(Ph)_3]$ (reaction 3) are shown in Figure 5b and Table I. The final product is characterized by bands at 444, 553, and 595 nm. Clear isosbestic points are observed at 440, 550, and 586 nm. Analyses of the spectral changes as a function of ligand concentration were again performed and led to plots of the type shown in Figure 6b. From this plot, a value of $\log K_2 = 2.04$ was calculated for CH_2Cl_2. The second triphenylphosphine complex formed was ESR-silent, and this implies that O_2^- has been replaced with a second triphenylphosphine ligand, as shown in eq 3. In addition, a further reaction of O_2^- must have occurred since this species is not detected in the ESR spectrum. However, the exact nature of this reaction is not known. The small value for K_2 is in part due to the steric hindrance induced by the two triphenylphosphine ligands. This is demonstrated by bonding with the less sterically hindered dimethylphenylphosphine, which forms $(TPP)Rh[P(CH_3)_2(C_6H_5)]_2^+$ by reaction with $(TPP)Rh(O_2)$.[21]

The titration of $(TPP)Rh(O_2)$ with triphenylphosphine in CH_2Cl_2 is independent of the presence of oxygen (air), and identical values of $\log K_1$ and $\log K_2$ were obtained in air-saturated solutions and in solutions under an argon atmosphere. In addition, formation of the triphenylphosphine bisadduct in THF was observed only at much larger mole ratios of triphenylphosphine than that in CH_2Cl_2. In benzonitrile $(TPP)Rh[P(Ph)_3]_2^+$ was not observed.

Conclusion

A simple MO diagram for $(P)Rh(O_2)$[3] describes the LUMO as a half-filled antibonding metal–O_2 orbital. The MO diagram formulated the Rh–O_2 bond as an ionic Rh^{III}–O_2^- mode. The electrochemical data presented in this paper qualitatively agree with this description of the LUMO. The first electron is added to a metal–axial ligand orbital (i.e. not porphyrin), followed by the loss of O_2^-. The electrochemical results, however, do not implicitly support the ionic bonding mode for the Rh–O_2 bond.

It is interesting to make a comparison of the electrochemical behavior of various rhodium tetraphenylporphyrin complexes. For (TPP)Rh(R) where R = $COCH_3$, CH_3, and CH_2Cl the first reduction potentials in methylene chloride (0.1 M TBAP) are −1.41, −1.44, and −1.50 V, respectively.[13,17] These reductions are reversible on the cyclic voltammetric time scale and appear to be at the porphyrin ligand. The differences between the first reduction potentials of the (TPP)Rh(R) compounds are relatively small. However, they are significantly more negative than for complexes of the type $[(TPP)Rh(L)_2]^+$. For example, in methylene chloride (0.1 M TBAP) at a scan rate of 100 mV/s the first reduction potentials for $(TPP)Rh[P(Ph_3)]_2^+$, $(TPP)Rh[NH(CH_3)_2]^+$, and $(TPP)Rh[NH(CH_3)_2]Cl$ are −0.98, −1.07, and −1.18 V, respectively. These reductions are metal-centered and are followed by loss of the axial ligand. Although the first reduction potential of the second set of complexes is dependent upon the rate of the following chemical reaction, they are shifted by about 300 mV positive compared to those of the (TPP)Rh(R) complexes. $(TPP)Rh(O_2)$ is reduced at −1.14 V in methylene chloride (0.1 M TBAP) at a scan rate of 100 mV/s. Again the reduction is metal-centered followed by loss of the axial ligand.

On the basis of the electrochemical results, the nature of the LUMO changes from a macrocycle orbital to a metal–axial ligand orbital with a change in axial ligand. The change in the nature of the LUMO is in basic agreement with results from an iterative extended Hückle calculation performed on the Rh(III) porphyrin species (P)Rh(py)Cl and (P)Rh(py)CN.[22] This calculation demonstrated that the LUMO in both cases is an orbital comprised primarily of the porphyrin $e_g(\pi^*)$ set. For (P)Rh(py)Cl, the molecular orbital comprised primarily of the metal d_{z^2} orbital is only about 1 eV above the LUMO, while for (P)Rh(py)CN the difference was found to be about 2.5 eV, indicating the effect of the axial ligand. However, our results indicate that, for complexes like (P)Rh(py)CN and (P)Rh(py)Cl, the LUMO should not be a porphyrin orbital. A different method of calculation of the MO diagram for these complexes may settle differences with the experimental results.

Acknowledgment. The support of the National Science Foundation (Grant No. CHE-8215507) is gratefully acknowledged.

Registry No. $(TPP)Rh(O_2)$, 71986-21-5; $[(TPP)Rh]_2$, 88083-37-8; $[(TPP)Rh]_2^{2-}$, 102747-23-9; $(TPP)Rh(O_2)[PPh_3]$, 102781-71-5; $(TPP)Rh[PPh_3]_2^+$, 102747-24-0; Rh, 7440-16-6; $(TPP)Rh(CH_2Cl)$, 100466-61-3.

(21) $(TPP)Rh[P(CH_3)_2(C_6H_5)]_2^+$ is characterized by bands in the UV–visible spectrum at 443, 555, and 594 nm. The ^1H NMR spectrum has the following peaks in $CDCl_3$: δ 2.85 ($P-CH_3$, triplet, 12 H), 6.97 (P–phenyl, triplet, 2 H), 6.45 (P–phenyl, triplet, 4 H), 3.83 (P–phenyl, multiplet, 4 H), besides normal porphyrin peaks. The infrared spectrum has no bands associated with Rh–O_2 but did have absorptions indicative of $P(CH_3)_2(C_6H_5)$. Finally, no ESR signal was observed for this compound.

(22) Antipas, A.; Gouterman, M. *J. Am. Chem. Soc.* **1983**, *105*, 4896.